

# Layered VOPO<sub>4</sub> as a Cathode Material for Rechargeable Zinc-Ion Battery: Effect of Polypyrrole Intercalation in the Host and Water Concentration in the Electrolyte

Vivek Verma,<sup>†</sup> Sonal Kumar,<sup>†</sup> William Manalastas Jr.,<sup>\*,†</sup> Jin Zhao,<sup>†</sup> Rodney Chua,<sup>†</sup> Shize Meng,<sup>†</sup> Pinit Kidkhunthod,<sup>‡</sup> and Madhavi Srinivasan<sup>\*,†</sup>

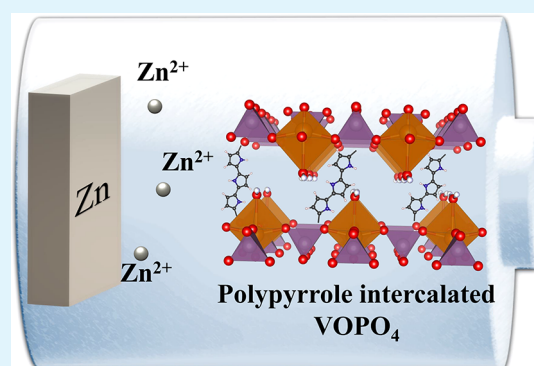
<sup>†</sup>School of Materials Science and Engineering, Nanyang Technological University, 50 Nanyang Avenue, 639798 Singapore

<sup>‡</sup>Synchrotron Light Research Institute (SLRI), Nakhon Ratchasima 30000, Thailand

## Supporting Information

**ABSTRACT:** Rechargeable zinc-ion batteries (RZIB) present an interesting alternative to rechargeable Li-ion batteries. Among the active materials, layered vanadium-based oxides show a poor cell voltage but modifying this structure by attaching a phosphate group to the vanadium redox center can drastically enhance the cathode voltage. With this layered VOPO<sub>4</sub> material, we demonstrate that preintercalating polypyrrole between crystallographic layers and using electrolyte with controlled water amounts are two absolutely essential conditions for easy and reversible Zn<sup>2+</sup> (de)intercalation, thus vastly improving battery outputs and long-term capacity retention. We establish that the rational design of open-layered structures hinges imperatively on factors like host structural integrity and electrode–electrolyte compatibility in delivering the performance of multivalent-ion batteries.

**KEYWORDS:** rechargeable zinc batteries, intercalation cathode, open layered structure, polypyrrole preintercalation, VOPO<sub>4</sub>



## INTRODUCTION

Although rechargeable Li-ion batteries are widely popular in the field of portable electronics, their application in the large-scale grid energy technologies are less attractive when considering cost, safety, and supply risk of Li metal.<sup>1–4</sup> In this regard, rechargeable batteries using other metal-ions are receiving increased attention.<sup>3–7</sup> Among the various alternative metals, zinc metal can be a good choice as an anode when compared to lithium because of (1) higher volumetric capacities,<sup>8</sup> (2) lower cost, and (3) possibility of transferring multiple charges per ion, when compared to lithium.<sup>3,5</sup>

Given the advantages of using zinc metal as an anode, developing a good cathode material for this anode is of immense interest. However, most studies suggest that intercalating multivalent-ions (including Zn<sup>2+</sup>) into the host structure is difficult when compared to Li<sup>+</sup> because of the high charge-to-size ratio of the multivalent-ions.<sup>9–11</sup> The higher charge-to-size ratio of a multivalent-ion strongly polarizes the host structure and limits its diffusivity inside the host structure.<sup>11</sup> Further, multivalent cations can also induce a heavy structural distortion causing the host structure to collapse as demonstrated by Park et al.<sup>12</sup> Hence, crystal structures with open frameworks which can both minimize the high electrostatic repulsion and buffer the steric destabilization are promising.<sup>11,13–17</sup>

Various studies have explored layered vanadium-based oxides as a RZIB cathode,<sup>3,18</sup> and these materials demonstrate

successful zinc-cation storage via an intercalation mechanism.<sup>14,19–21</sup> These materials possess a high interlayer spacing created by various preintercalated cations or water molecules.<sup>22</sup> The high interlayer spacing can minimize the electrostatic repulsion between host material and the intercalating cation, thus easing the multivalent-cation intercalation.<sup>14,23</sup> In addition, the intercalated water molecules/cations act as “pillars”, preserving the structural integrity of the host structure during (de)intercalation.<sup>24,25</sup> However, the intercalation voltage of this class of oxide materials is low, roughly at 0.7 V vs Zn<sup>2+</sup>/Zn.<sup>3,18</sup>

A phosphate group linked to the vanadium-ion center can enhance the cation intercalation voltage as compared to the vanadium oxides via an inductive effect.<sup>26</sup> VOPO<sub>4</sub>·2H<sub>2</sub>O is a material that exists as a layered phase with a high interlayer spacing.<sup>27</sup> The high interlayer spacing, created by the preintercalated water molecules between the VOPO<sub>4</sub> layers, can minimize the electrostatic repulsion between the intercalating Zn<sup>2+</sup> and the host structure and, hence, can make the Zn<sup>2+</sup> migration inside the host easy. However, we observed a rapid capacity fade and a structural change in the host during repeated zinc (de)intercalation. On preintercalating polypyrrole between the VOPO<sub>4</sub> layers, we observe that

**Received:** August 21, 2019

**Accepted:** October 28, 2019

**Published:** October 28, 2019

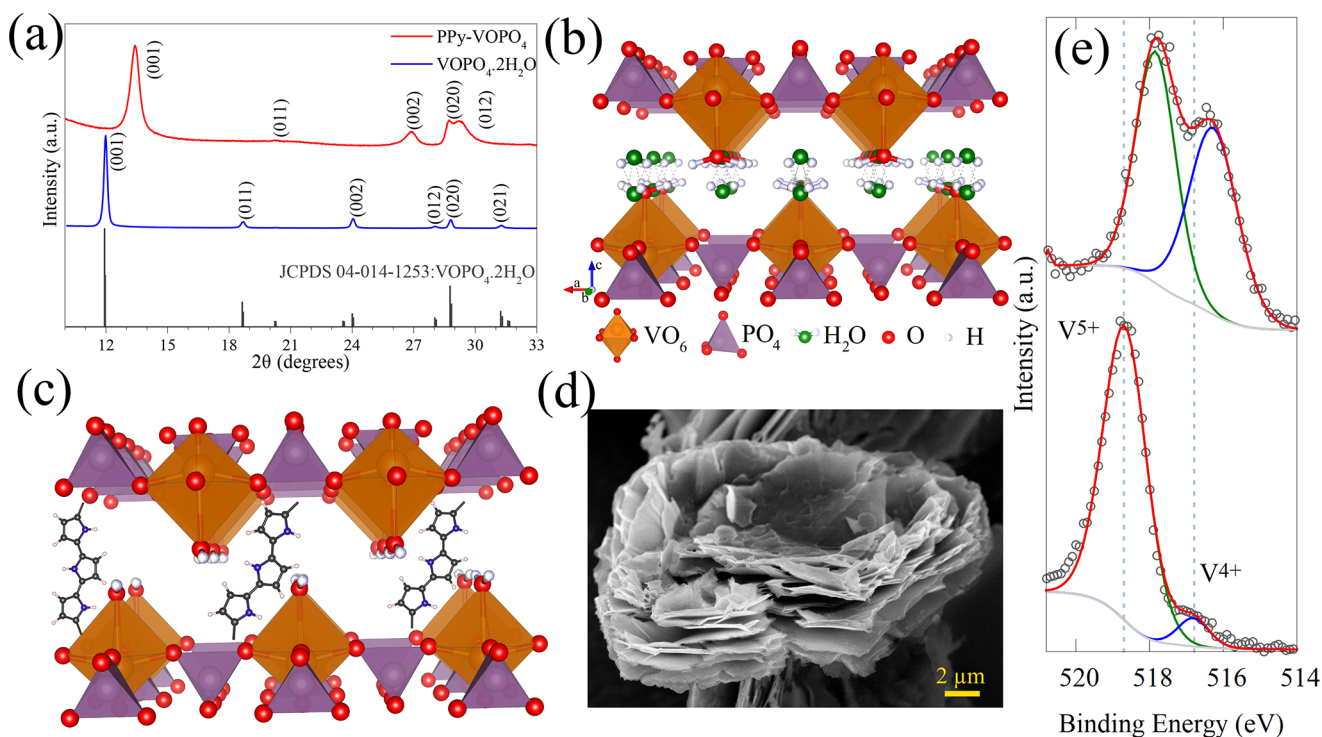


**Figure 1.** (a) XRD patterns for synthesized  $\text{VOPO}_4 \cdot 2\text{H}_2\text{O}$  and  $\text{PPy-VOPO}_4$ . (b) Crystal structure of  $\text{VOPO}_4 \cdot 2\text{H}_2\text{O}$  (c) schematic for  $\text{PPy-VOPO}_4$  showing the polypyrrole units intercalated between the  $\text{VOPO}_4$  layers, (d) layered stacks of  $\text{PPy-VOPO}_4$  in an SEM image, and (e) V  $2p_{3/2}$  XPS spectra for  $\text{VOPO}_4 \cdot 2\text{H}_2\text{O}$  (bottom) and  $\text{PPy-VOPO}_4$  (top).

the cycling stability improves, and therefore, we study polypyrrole-intercalated  $\text{VOPO}_4$  ( $\text{PPy-VOPO}_4$ ) as a cathode host material for RZIB. Moreover, for using the  $\text{Zn}(\text{CF}_3\text{SO}_3)_2/\text{acetonitrile}$  electrolyte with the  $\text{VOPO}_4$ -based cathode for RZIB, Wang et al. have showed the benefits of adding low-amounts of water to the electrolyte for improving the battery performance.<sup>28</sup> However, the problems associated with adding high-amounts of water were not elaborated on. We find that there is a problem of severe cathode-material dissolution which in turn affects the cycling stability. By a similar vein, we demonstrate that an optimum water amount in the electrolyte is needed to maximize the battery capacity and the cycling stability for this cathode material. With the optimized electrolyte, the battery could demonstrate a high average voltage of 1.1 V vs  $\text{Zn}^{2+}/\text{Zn}$ , along with a maximum capacity of  $86 \text{ mAh g}^{-1}$  and cycling stability of 350 cycles. Finally, using a combination of XRD and XPS techniques, we elucidate the zinc storage mechanism for this system.

## RESULTS AND DISCUSSION

The X-ray diffractogram for the synthesized  $\text{VOPO}_4 \cdot 2\text{H}_2\text{O}$  (Figure 1a) matches well with the database (JCPDS 04-014-1253).<sup>29</sup> Tachez et al.<sup>30</sup> have described the crystal structure (Figure 1b) as a structure consisting of  $\text{VOPO}_4$  layers wherein each vanadium-ion center is bonded to six O atoms with slightly different bond lengths and thus forms a distorted  $\text{VO}_6$  octahedra (shown as orange octahedra). Four of these V–O bonds, where O atoms are shared to phosphate tetrahedra (purple tetrahedra), lie in the equatorial or a-b plane. One of the axial bonds is formed with an O atom which is slightly shorter than the equatorial V–O bond length, while the other axial V–O bond is elongated as two H atoms are attached to this O atom, similar to a water molecule (red sphere bonded to

two white spheres). Notably, this structure gives rise to extended hydrogen-bonding networks allowing for discrete water molecules to reside within the  $\text{VOPO}_4$  layers (where O atom is represented in green). These  $\text{H}_2\text{O}$  molecules are weakly bonded and can be easily removed.<sup>27</sup>

The XRD pattern for the synthesized  $\text{PPy-VOPO}_4$  (Figure 1a) matches well with previous reports.<sup>31,32</sup> While all the peak positions for the “ $l$ ”-dependent  $hkl$  planes shift to higher  $2\theta$  angles after polypyrrole intercalation, the “ $l$ ”-independent (020) plane does not shift, indicating that only the unit cell dimension along the direction perpendicular to the  $\text{VOPO}_4$  layers ( $c$ -axis) contracts. This observation is consistent with the argument made by Benes et al. that most of the intercalating species leave the  $\text{VOPO}_4$  layers unaltered and only change the  $\text{VOPO}_4$  interlayer separation (Figure 1c).<sup>27</sup> The reduction in the “ $c$ ” unit cell length leads to a decrease in the spacing between the  $\text{VOPO}_4$  layers from  $7.43 \text{ \AA}$  (in  $\text{VOPO}_4 \cdot 2\text{H}_2\text{O}$ ) to  $6.72 \text{ \AA}$ , calculated using (001) planes. Although intercalating most organic species between the  $\text{VOPO}_4$  layers increases the  $\text{VOPO}_4$  layer spacing, a few species including polypyrrole have been shown to decrease the interlayer separation after intercalation (Table S1).<sup>31</sup> De et al. have suggested that the reduction in the interplanar spacing could be due to the replacement of weakly bonded water molecules with polypyrrole units.<sup>32</sup> The overlap of the (020) and (012) planes, which has also been observed previously with polypyrrole intercalation into  $\text{VOPO}_4$ , can be ascribed to the fact that all the XRD peaks are much broader after intercalating polypyrrole as the crystallite size reduces after polypyrrole intercalation.<sup>32</sup>

The SEM micrograph for  $\text{PPy-VOPO}_4$  (Figure 1d) indicates that the material consists of an irregular stack of sheets, unlike the orderly stacked layers of  $\text{VOPO}_4 \cdot 2\text{H}_2\text{O}$  (Figure S1). This

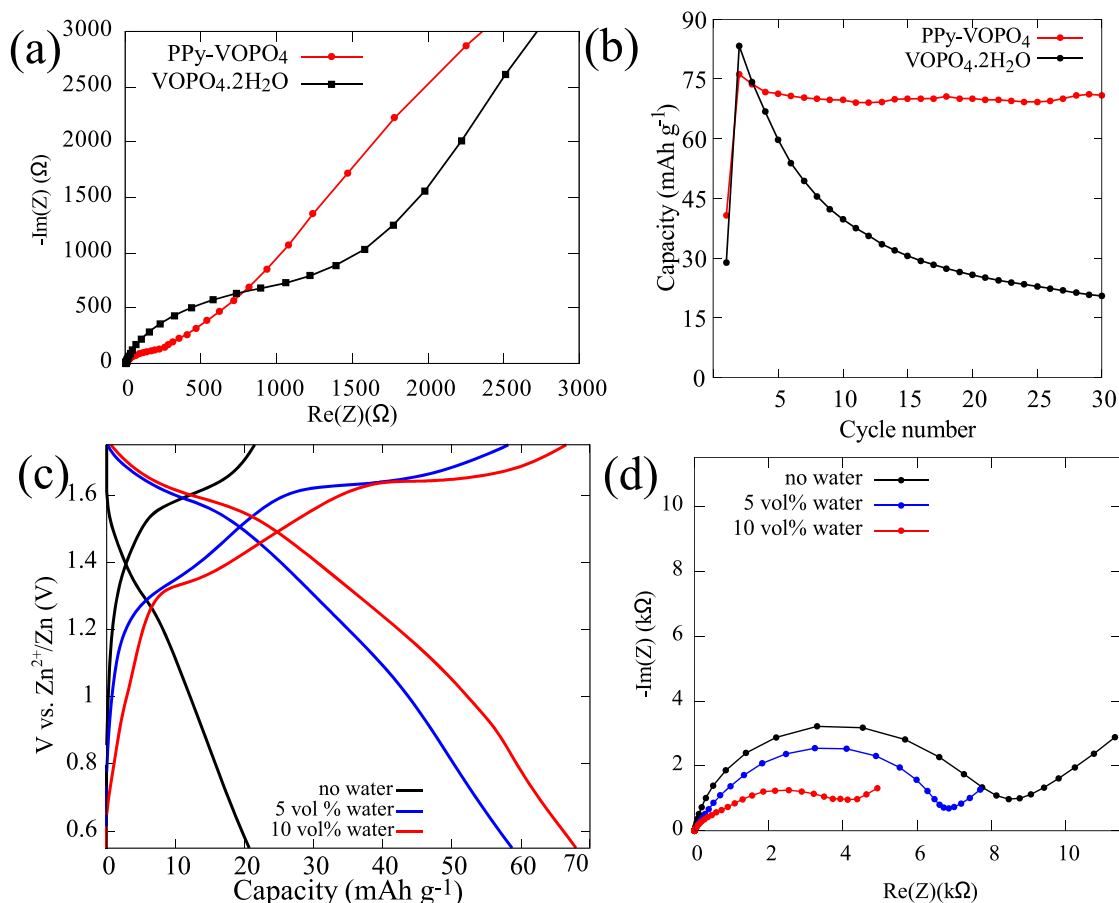


**Figure 2.** (a) EIS spectra for RZIB using  $\text{VOPO}_4 \cdot 2\text{H}_2\text{O}$  or PPy- $\text{VOPO}_4$  as a cathode material, (b) comparison of the cycling stabilities for  $\text{VOPO}_4 \cdot 2\text{H}_2\text{O}$  and PPy- $\text{VOPO}_4$  at a current rate of  $30 \text{ mA g}^{-1}$  in  $1 \text{ M Zn}(\text{CF}_3\text{SO}_3)_2/\text{acetonitrile}$  electrolyte with  $10 \text{ vol} \%$  water. (c) Charge–discharge curve of second cycles and (d) EIS spectra for PPy- $\text{VOPO}_4$  RZIB in  $\text{Zn}(\text{CF}_3\text{SO}_3)_2/\text{acetonitrile}$  electrolyte with different water concentrations.

observation is consistent with the XRD results, wherein the broadening of ( $00l$ ) type peaks after polypyrrole intercalation indicates that the crystallite size along the axis normal to the  $\text{VOPO}_4$  layers is reduced.<sup>33</sup> Polypyrrole intercalation changes the color of powder from bright yellow to dark green (Figure S2).<sup>34</sup> The presence of polypyrrole in the host was confirmed by FTIR (Figure S3), and the chemical composition of the final material as determined by using TGA and CHN analyzer is  $(\text{PPy})_{0.4}\text{VOPO}_4 \cdot 1.17 \text{ H}_2\text{O}$  (Figure S4 and Table S2).

The chemical interaction between the intercalated polypyrrole and the  $\text{VOPO}_4$  layers was further illustrated in the XPS results (Figure 1e). Before the polypyrrole intercalation, V in the material shows mostly the  $5+$  oxidation state at an energy of  $518.7 \text{ eV}$  along with a small amount in the  $4+$  oxidation state at  $516.8 \text{ eV}$ .<sup>35,36</sup> However, after the polypyrrole intercalation: (1) the relative ratio of  $\text{V}^{4+}/\text{V}^{5+}$  increases, indicating that the vanadium-ions exist in a mixed oxidation state of  $\text{V}^{4+}/5+$ . The existence of mixed oxidation state of V was also confirmed by V K-edge XANES spectra which showed that the average oxidation state of V lies between  $4+$  and  $5+$  (Figure S5). (2) Both the peaks shift to lower binding energies with the host intercalation by polypyrrole, a phenomenon which has also been observed during layered  $\text{VOPO}_4$  host intercalation by other carbon materials.<sup>36</sup>

The mixed valency of the V-ion center enhances the electronic conductivity of the PPy- $\text{VOPO}_4$  host structure when compared to  $\text{VOPO}_4 \cdot 2\text{H}_2\text{O}$  (Figure S6)<sup>32,37</sup> because the electron charge cloud can be delocalized between adjacent V-

ions when present in the mixed oxidation state.<sup>38,39</sup> Intercalated polypyrrole also improves the electronic conductivity as it is partially present in its oxidized state when intercalated between  $\text{VOPO}_4$  layers.<sup>31,32</sup> Due to the improved electronic conductivity, the semicircle in the EIS spectra, which Kundu et al. ascribed to the charge-transfer resistance at the electrode–electrolyte interface,<sup>24</sup> is smaller for PPy- $\text{VOPO}_4$  as compared to  $\text{VOPO}_4 \cdot 2\text{H}_2\text{O}$  (Figure 2a and Figure S7).

Additionally, polypyrrole intercalation between the  $\text{VOPO}_4$  layers benefits the structural integrity as it acts as a better pillaring unit when compared to water. For  $\text{VOPO}_4 \cdot 2\text{H}_2\text{O}$ , a drastic capacity fading is observed during charge/discharge (Figure 2b and Figure S8). Ex-situ XRD (Figure S8c) for the cycled electrodes revealed that the interplanar spacing between the  $\text{VOPO}_4$  layers reduce over repeated cycling, which can be ascribed to the loss of the hydrogen-bonded water molecules from the host structure.<sup>27,33</sup> On the other hand, the capacity retention showed a drastic improvement in the case of PPy- $\text{VOPO}_4$  (from  $25\%$  to  $90\%$  in 30 cycles, Figure 2b and Figure S9). A similar improvement in the capacity retention was also observed when Wei et al. preintercalated some charged cations between the layered structure of vanadium oxide.<sup>40</sup> Wei et al. explained that the intercalating species holds the layered structure intact and reduces the structural distortion in the host structure during repeated (de)intercalation.

While our aim was to use a water-solvent based electrolyte for testing the PPy- $\text{VOPO}_4$  as the RZIB cathode material, a purely aqueous electrolyte could not be used as the PPy-

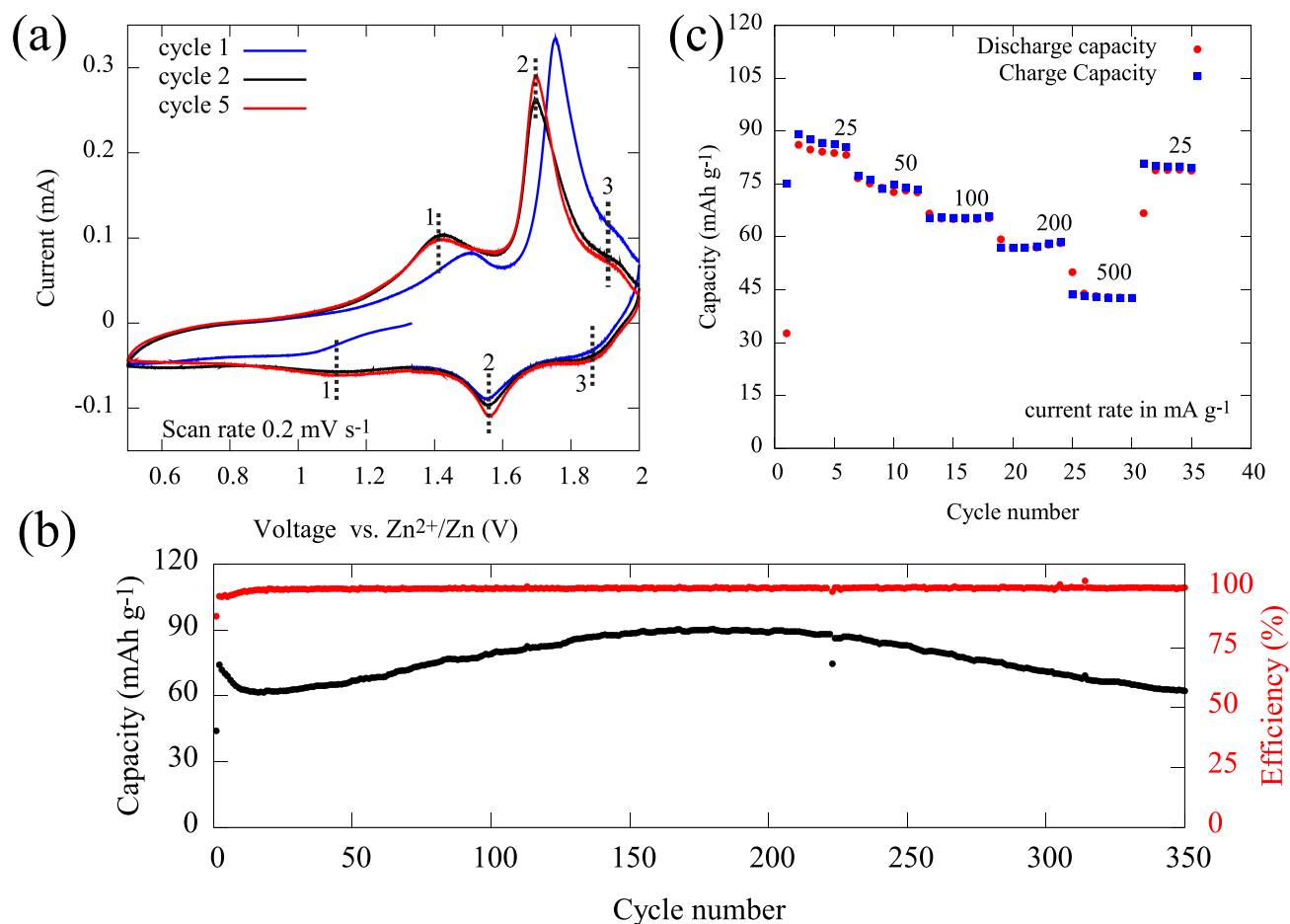


**Figure 3.** (a) Cyclic voltammetry for PPy-VOPO<sub>4</sub> RZIB in 1 M Zn(CF<sub>3</sub>SO<sub>3</sub>)<sub>2</sub>/acetonitrile electrolyte with 10 vol % water; each pair of peaks is marked with a dashed line and assigned a numerical identifier. (b) Battery cycling performance at 0.1 A g<sup>-1</sup> and (c) rate capability for PPy-VOPO<sub>4</sub> RZIB in 1 M Zn(CF<sub>3</sub>SO<sub>3</sub>)<sub>2</sub>/acetonitrile electrolyte with 10 vol % water.

VOPO<sub>4</sub> material slowly dissolves in water (Figure S10). Therefore, an acetonitrile solvent-based electrolyte was used. However, without any addition of water in the acetonitrile-based electrolyte, the battery could show hardly any capacity (Figure 2c). On adding small amounts of water to the electrolyte, we see an improvement in the capacities. A similar trend in the capacity improvement was also observed for the case of VOPO<sub>4</sub>·2H<sub>2</sub>O (Figure S11b).

To investigate why the addition of water in the electrolyte increases the capacity, we measured the EIS impedance spectrum for the VOPO<sub>4</sub>-based battery system with varying water amounts (Figure 2d). We observed a reduction in the semicircle diameter on increasing the water concentration in the electrolyte. Kundu et al. had previously ascribed the semicircle to the charge-transfer impedance at the electrode–electrolyte interface, specifically to the energy penalties involved in desolvating Zn<sup>2+</sup> from its solvation shell during Zn<sup>2+</sup> charge transfer at either the cathode or the anode.<sup>24</sup> Studies have found that the energy penalty to desolvate a multivalent-ion is much lower in water when compared to solvents like acetonitrile or propylene carbonate.<sup>24,41</sup> This is also evident in the broadening of the CV peaks in the system without any added water in the electrolyte and indicates sluggish kinetics (Figure S12).<sup>37</sup> Similar to the PPy-VOPO<sub>4</sub> system, we find the same trend of broadened CV peaks and reduced capacities in a water-free electrolyte for VOPO<sub>4</sub>·2H<sub>2</sub>O, again indicating poor kinetics (Figure S11).

While adding a small amount of water in the electrolyte is beneficial, increasing the water amounts beyond 10 vol % is detrimental. Adding a higher water amount leads to a marginal increase in the capacity but deteriorates the capacity retention due to the PPy-VOPO<sub>4</sub> material dissolution in the water (Figure S13). Therefore, a trade-off exists between (1) increasing the water content in the electrolyte to reduce zinc cation desolvation energies at the electrolyte–electrode interface and (2) decreasing the electrolyte water content to limit the cathode material dissolution. Based on the capacities and cycling performance of the Zn/PPy-VOPO<sub>4</sub> system with different electrolytes, we find the electrolyte with 10 vol % water to be the optimum and investigate this system in detail.

The cyclic voltammogram (Figure 3a) for PPy-VOPO<sub>4</sub> in 10 vol % water electrolyte shows three pairs of oxidation–reduction peaks. A similar CV profile with multiple peaks was also observed for VOPO<sub>4</sub>-based cathode for Li, Mg, and K systems,<sup>37,42,43</sup> and the appearance of multiple peaks was attributed to the guest cation insertion in multiple stages.<sup>42</sup> We also note that the polypyrrole itself, when used as a cathode material, does not give any redox peak in CV (Figure S14a).

The Galvanostatic charge–discharge (GCD) test at a high current rate of 0.1 A g<sup>-1</sup> shows a good cycling stability up to 350 cycles (Figure 3b). We report an unprecedented operational lifetime of 455 h, surpassing the other reported works on VOPO<sub>4</sub>-based ZIAB (Table S3), indicating that the cathode material dissolution over an extended period of time is

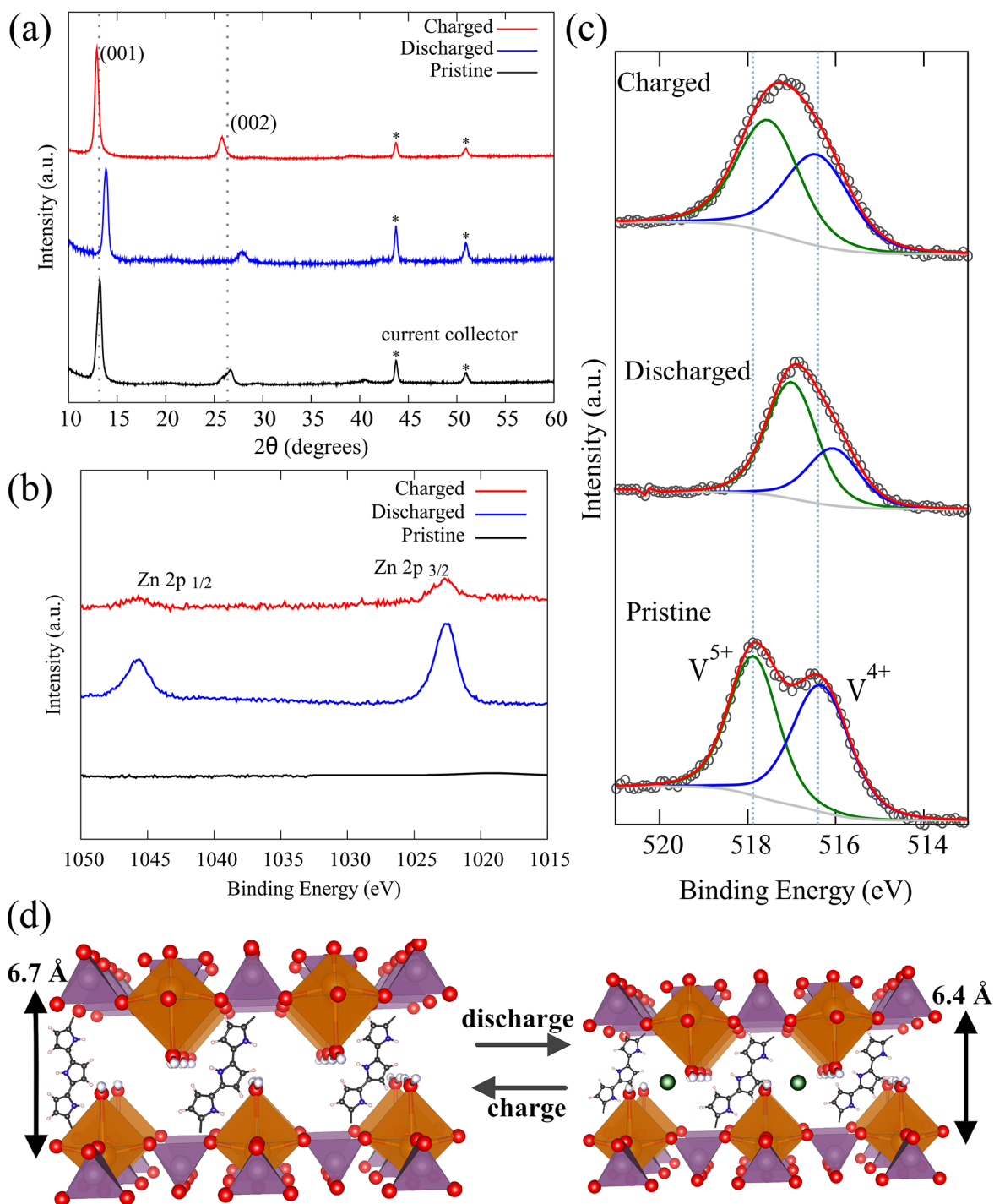


**Figure 4.** (a) Ex situ XRD of PPy-VOPO<sub>4</sub> cathode showing shifts in the (00*l*) type planes at various stages of charging. XPS spectra for (b) Zn 2p peaks and (c) V 2p<sub>3/2</sub> during different states of charging. (d) Schematic depicting overall mechanism of zinc (de)intercalation into the PPy-VOPO<sub>4</sub> host structure. Green spheres indicate Zn<sup>2+</sup> ions.

much lower in our system. We note that the capacity values decrease initially in the first few cycles and then subsequently increase, similar to other reported works.<sup>25,44,45</sup> The initial capacity drop has been attributed to the fact that during the discharging step, some Zn<sup>2+</sup> ions intercalated in the host structure remain in the host structure as “dead Zn<sup>2+</sup> sites” and cannot be fully extracted during the charging step. The subsequent capacity rise has been ascribed to the gradual activation of the electrodes by other reports on RZIB.<sup>21,25</sup> Notably, the capacity rise during the gradual activation regime

was significant ( $\approx 50\%$ ) and lasted for nearly 200 cycles. This slow and long activation has also previously been observed in the Zn(CF<sub>3</sub>SO<sub>3</sub>)<sub>2</sub>/acetonitrile electrolyte systems and was attributed to both sluggish kinetics in the electrolyte and a decrease in charge transfer impedance at the zinc anode via progressive electrochemical polishing.<sup>24</sup> The rate performance of the battery (Figure 3c) demonstrates that the maximum discharge capacities achieved at a current rate of 25, 50, 100, 200, 500 mA/g are 86, 76, 65, 57, and 43 mAh/g, respectively. When the current is returned to the rate of 25 mA/g, the

battery could still achieve a discharge capacity of 78 mA/g, which is 90.6% of the initial capacity. We also note that the polypyrrole shows a very limited capacity contribution (Figure S14b).

To gain insights into the host material intercalation behavior, we take ex situ XRD of the cathode material in the charged and discharged states of the fifth cycle (Figure 4a). We note that the X-ray diffraction patterns of the electrodes show a preferential orientation along the (00 $l$ ) type planes which can be ascribed to the PPy-VOPO<sub>4</sub> sheets orienting parallel to the electrode surface after electrode fabrication. As shown in Figure 4a, the shifts in the (001) and (002) planes to higher  $2\theta$  angles in the discharged sample indicate an interlayer contraction as compared to the pristine sample. The interlayer layer spacing, as estimated using the (001) plane, shrinks from 6.72 to 6.39 Å. This contraction in the interlayer spacing was also observed when Zn<sup>2+</sup> is intercalated in other layered materials.<sup>14,19,25</sup> The reason was ascribed to the electrostatic attraction between the guest Zn<sup>2+</sup> cation and the host material layers, pulling the layers close to each other. When the cathode material is charged, the (001) and (002) planes again shift to lower  $2\theta$  angles and closely resemble the diffractogram of the pristine sample. We note that even after a charging/discharging of 100 cycles, the host structure can retain its layered structure (Figure S15). The (001) interplanar spacing is 6.14 Å in the 100th discharged state which implies that the host structure is still electrochemically active and intercalates Zn-ions. This interplanar spacing is slightly lower than the 6.39 Å spacing observed for the fifth discharge cycle suggesting more zinc cations are stored in the host and is consistent with an increase in the capacity observed in the later cycles after the initial electrochemical activation (Figure S13).

XPS further supports the zinc intercalation phenomena into the host structure. The Zn 2p XPS spectra in the pristine, charged, and discharged states of the cathode material are shown in Figure 4b. While no zinc is present in the pristine electrode, Zn 2p<sub>3/2</sub> (1022.07 eV) and Zn 2p<sub>1/2</sub> (1045.27 eV) peaks appear in the discharged state, indicating the presence of Zn<sup>2+</sup> species. Further, when the electrode is charged, the zinc peak intensities reduce, indicating that most of the zinc cations have been extracted out of the cathode material. However, we also note that some residual amount of Zn<sup>2+</sup> species still remains inside the host structure after charging, even when the interlayer spacing is observed to be restored from the XRD results. This observation is consistent with the studies made by Kundu et al. where the authors observed that a small quantity of Zn<sup>2+</sup> ions are trapped in the host vanadium oxide structure in the first cycle, and thereafter the slightly modified host structure shows a reversible Zn<sup>2+</sup> (de)intercalation.<sup>24</sup>

Vanadium XPS spectra provides further evidence of the zinc (de)intercalation inside the host (Figure 4c). The pristine electrode showed two peaks present in the sample at the binding energy values of 517.8 and 516.3 eV. When the electrode was discharged, both the peaks showed a red shift to the values of 517.1 and 516.0 eV, respectively, indicating a reduction of the vanadium-ion centers during Zn<sup>2+</sup> intercalation. When the electrode was charged, both the peaks are blue-shifted from the discharged electrode values to the final values of 517.5 and 516.3 eV, respectively. However, we note that the final peak position of the V<sup>5+</sup> model peak in the charged state was slightly red-shifted compared to the pristine sample, indicating that not all the vanadium-ion centers were oxidized back during the charging process. This can be

ascribed to the fact that some Zn<sup>2+</sup>-ions remain trapped in the host structure after charging; therefore, the vanadium-ion environment is modified in the charged electrode as compared to the pristine electrode.

Therefore, based on the structural characterization studies, we can deduce the following mechanism (Figure 4d). During discharging, the vanadium-ion centers reduce as zinc cations intercalate into the host structure. The intercalated zinc cations pull the VOPO<sub>4</sub> layers close to each other via the electrostatic attractive forces. During charging, the vanadium-ion centers oxidize again as the zinc cations are deintercalated from the host structure, and the VOPO<sub>4</sub> layers restore their original separation. However, few zinc cations remain trapped inside the host structure and thus the vanadium-ion environment cannot fully revert to the original state.

## CONCLUSIONS

In conclusion, we demonstrate that PPy-VOPO<sub>4</sub> can deliver a high average discharge voltage of 1.1 V vs Zn<sup>2+</sup>/Zn as a RZIB cathode. From the host material's perspective, a high interlayer spacing between the VOPO<sub>4</sub> layers made Zn<sup>2+</sup> cation (de)intercalation feasible. However, only after the polypyrrole intercalation between the VOPO<sub>4</sub> layers, a high structural stability was achieved and the battery could perform reversibly up to 350 cycles. From the electrolyte perspective, we observed that contrary to the popular belief, an aqueous electrolyte might not always be better than a nonaqueous electrolyte as it might lead to problems like the electrode material dissolution. On the other hand, a nonaqueous electrolyte might not also be the best choice due to poor kinetics, and the choice of the electrolyte is subjective to the electrode material. These findings will help us in designing better cathode and electrolyte materials not only for zinc-ions but in general for all multivalent-ions.

## ASSOCIATED CONTENT

### Supporting Information

The Supporting Information is available free of charge at <https://pubs.acs.org/doi/10.1021/acsaem.9b01632>.

Experimental section, synthesis procedure and additional characterization details (TGA, CHN analysis, XANES, ex situ XRD, and cyclic voltammetry) (PDF)

## AUTHOR INFORMATION

### Corresponding Authors

\*E-mail: [wmanalastas@ntu.edu.sg](mailto:wmanalastas@ntu.edu.sg).

\*E-mail: [madhavi@ntu.edu.sg](mailto:madhavi@ntu.edu.sg).

### ORCID

Vivek Verma: 0000-0002-4890-2826

William Manalastas, Jr.: 0000-0002-2364-0604

### Notes

The authors declare no competing financial interest.

## ACKNOWLEDGMENTS

This work was funded by the National Research Foundation of Singapore Investigatorship Award Number NRFI2017-08/NRF2016NRF-NRFI001-22. V.V would like to thank Fang Yanan and Sai S. H. Dintakurti for a fruitful discussion on XRD analysis, Teddy Salim for XPS analysis, Disha Gupta and Suchinda Sattayaporn for XANES analysis, Tan Han Khiang for CHN analysis, and Yi Cai, Du Yuan, and Hao Ren for help

in designing electrochemical experiments. The authors thank Synchrotron Light Research Institute (BLS.2), Nakhon Ratchasima, Thailand, for XANES measurements and the Facility for Analysis, Characterization, Testing and Simulation, Nanyang Technological University, Singapore, for use of their electron microscopy/X-ray facilities.

## REFERENCES

- (1) Wanger, T. C. The Lithium future-resources, recycling, and the environment. *Conservation Letters* **2011**, *4*, 202–206.
- (2) Helbig, C.; Bradshaw, A. M.; Wietschel, L.; Thorenz, A.; Tuma, A. Supply risks associated with lithium-ion battery materials. *J. Cleaner Prod.* **2018**, *172*, 274–286.
- (3) Verma, V.; Kumar, S.; Manalastas, W., Jr.; Satish, R.; Srinivasan, M. Progress in Rechargeable Aqueous Zinc-and Aluminum-Ion Battery Electrodes: Challenges and Outlook. *Advanced Sustainable Systems* **2019**, *3*, 1800111.
- (4) Yuan, D.; Manalastas, W., Jr.; Zhang, L.; Chan, J. J.; Meng, S.; Chen, Y.; Srinivasan, M. Lignin@ Nafion Membranes Forming Zn Solid–Electrolyte Interfaces Enhance the Cycle Life for Rechargeable Zinc-Ion Batteries. *ChemSusChem* **2019**, *12*, 4889.
- (5) Manalastas, W., Jr.; Kumar, S.; Verma, V.; Zhang, L.; Yuan, D.; Srinivasan, M. Water in rechargeable multivalent-ion batteries: an electrochemical Pandora's box. *ChemSusChem* **2019**, *12*, 379–396.
- (6) Kumar, S.; Satish, R.; Verma, V.; Ren, H.; Kidkhunthod, P.; Manalastas, W.; Srinivasan, M. Investigating FeVO<sub>4</sub> as a cathode material for aqueous aluminum-ion battery. *J. Power Sources* **2019**, *426*, 151–161.
- (7) Chua, R.; Cai, Y.; Kou, Z. K.; Satish, R.; Ren, H.; Chan, J. J.; Zhang, L.; Morris, S. A.; Bai, J.; Srinivasan, M. 1.3 V superwide potential window sponsored by Na-Mn-O plates as cathodes towards aqueous rechargeable sodium-ion batteries. *Chem. Eng. J.* **2019**, *370*, 742–748.
- (8) Haynes, W. M. *CRC Handbook of Chemistry and Physics*; CRC Press, 2014; pp 8–20.
- (9) Levi, E.; Gofer, Y.; Aurbach, D. On the way to rechargeable Mg batteries: the challenge of new cathode materials. *Chem. Mater.* **2010**, *22*, 860–868.
- (10) Whittingham, M. S.; Siu, C.; Ding, J. Can multielectron intercalation reactions be the basis of next generation batteries? *Acc. Chem. Res.* **2018**, *51*, 258–264.
- (11) Rong, Z.; Malik, R.; Canepa, P.; Sai Gautam, G.; Liu, M.; Jain, A.; Persson, K.; Ceder, G. Materials design rules for multivalent ion mobility in intercalation structures. *Chem. Mater.* **2015**, *27*, 6016–6021.
- (12) Park, M. J.; Yaghoobnejad-Asl, H.; Therese, S.; Manthiram, A. Structural Impact of Zn-insertion into Monoclinic V<sub>2</sub>(PO<sub>4</sub>)<sub>3</sub>: Implications for Zn-ion Batteries. *J. Mater. Chem. A* **2019**, *7*, 7159–7167.
- (13) Zhao, J.; Ren, H.; Liang, Q.; Yuan, D.; Xi, S.; Wu, C.; Manalastas, W., Jr.; Ma, J.; Fang, W.; Zheng, Y.; Du, C.-F.; Srinivasan, M.; Yan, Q. High-performance flexible quasi-solid-state zinc-ion batteries with layer-expanded vanadium oxide cathode and zinc/stainless steel mesh composite anode. *Nano Energy* **2019**, *62*, 94–102.
- (14) Kundu, D.; Adams, B. D.; Duffort, V.; Vajargah, S. H.; Nazar, L. F. A high-capacity and long-life aqueous rechargeable zinc battery using a metal oxide intercalation cathode. *Nat. Energy* **2016**, *1*, 16119.
- (15) Knight, J. C.; Therese, S.; Manthiram, A. Chemical extraction of Zn from ZnMn<sub>2</sub>O<sub>4</sub>-based spinels. *J. Mater. Chem. A* **2015**, *3*, 21077–21082.
- (16) Li, H.; Yang, Q.; Mo, F.; Liang, G.; Liu, Z.; Tang, Z.; Ma, L.; Liu, J.; Shi, Z.; Zhi, C. MoS<sub>2</sub> nanosheets with expanded interlayer spacing for rechargeable aqueous Zn-ion batteries. *Energy Storage Materials* **2019**, *19*, 94–101.
- (17) Huang, J.; Wang, Z.; Hou, M.; Dong, X.; Liu, Y.; Wang, Y.; Xia, Y. Polyaniline-intercalated manganese dioxide nanolayers as a high-performance cathode material for an aqueous zinc-ion battery. *Nat. Commun.* **2018**, *9*, 2906.
- (18) Song, M.; Tan, H.; Chao, D.; Fan, H. J. Recent Advances in Zn-Ion Batteries. *Adv. Funct. Mater.* **2018**, *28*, 1802564.
- (19) Soundharajan, V.; Sambandam, B.; Kim, S.; Alfaruqi, M. H.; Putro, D. Y.; Jo, J.; Kim, S.; Mathew, V.; Sun, Y.-K.; Kim, J. Na<sub>2</sub>V<sub>6</sub>O<sub>16</sub>·3H<sub>2</sub>O barnesite nanorod: an open door to display a stable and high energy for aqueous rechargeable Zn-ion batteries as cathodes. *Nano Lett.* **2018**, *18*, 2402–2410.
- (20) Xia, C.; Guo, J.; Li, P.; Zhang, X.; Alshareef, H. N. Highly Stable Aqueous Zinc-Ion Storage Using a Layered Calcium Vanadium Oxide Bronze Cathode. *Angew. Chem., Int. Ed.* **2018**, *57*, 3943–3948.
- (21) Zhang, N.; Dong, Y.; Jia, M.; Bian, X.; Wang, Y.; Qiu, M.; Xu, J.; Liu, Y.; Jiao, L.; Cheng, F. Rechargeable Aqueous Zn-V<sub>2</sub>O<sub>5</sub> Battery with High Energy Density and Long Cycle Life. *ACS Energy Letters* **2018**, *3*, 1366–1372.
- (22) Clites, M.; Pomerantseva, E. Bilayered vanadium oxides by chemical pre-intercalation of alkali and alkali-earth ions as battery electrodes. *Energy Storage Materials* **2018**, *11*, 30–37.
- (23) Novak, P.; Desilvestro, J. Electrochemical insertion of magnesium in metal oxides and sulfides from aprotic electrolytes. *J. Electrochem. Soc.* **1993**, *140*, 140–144.
- (24) Kundu, D.; Hosseini Vajargah, S.; Wan, L.; Adams, B.; Prendergast, D.; Nazar, L. F. Aqueous vs. nonaqueous Zn-ion batteries: consequences of the desolvation penalty at the interface. *Energy Environ. Sci.* **2018**, *11*, 881–892.
- (25) Alfaruqi, M. H.; Mathew, V.; Song, J.; Kim, S.; Islam, S.; Pham, D. T.; Jo, J.; Kim, S.; Baboo, J. P.; Xiu, Z.; Lee, K.-S.; Sun, Y.-K.; Kim, J. Electrochemical Zinc Intercalation in Lithium Vanadium Oxide: A High-Capacity Zinc-Ion Battery Cathode. *Chem. Mater.* **2017**, *29*, 1684–1694.
- (26) Sun, Y.; Wu, C.; Xie, Y. Sonochemical synthesis of nanostructured VOPO 4·2H<sub>2</sub>O/carbon nanotube composites with improved lithium ion battery performance. *J. Nanopart. Res.* **2010**, *12*, 417–427.
- (27) Beneš, L.; Melanova, K.; Svoboda, J.; Zima, V. Intercalation chemistry of layered vanadyl phosphate: a review. *J. Inclusion Phenom. Mol. Recognit. Chem.* **2012**, *73*, 33–53.
- (28) Wang, F.; Sun, W.; Shadik, Z.; Hu, E.; Ji, X.; Gao, T.; Yang, X.-Q.; Xu, K.; Wang, C. How Water Accelerates Bivalent Ion Diffusion at the Electrolyte/Electrode Interface. *Angew. Chem., Int. Ed.* **2018**, *57*, 11978–11981.
- (29) Tietze, H. R. The crystal and molecular structure of oxovanadium (V) orthophosphate dihydrate, VOPO<sub>4</sub>·2H<sub>2</sub>O. *Aust. J. Chem.* **1981**, *34*, 2035–2038.
- (30) Tachez, M.; Theobald, F.; Bernard, J.; Hewat, A. Intercalation Of Water Molecules in a layer structure of vanadyl phosphate. Crystal structure of vanadyl phosphate dihydrate. *Rev. Chem. Miner.* **1982**, *19*, 291–300.
- (31) De Stefanis, A.; Foglia, S.; Tomlinson, A. A. Assembly and polymerisation of some aromatic amines in α-VOPO<sub>4</sub>·2H<sub>2</sub>O. *J. Mater. Chem.* **1995**, *5*, 475–483.
- (32) De, S.; Dey, A.; De, S. Characterization and electrical properties of vanadyl phosphate-polypyrrole nanocomposites. *J. Phys. D: Appl. Phys.* **2006**, *39*, 500.
- (33) Dupre, N.; Gaubicher, J.; Angenault, J.; Querton, M. Electrochemical study of intercalated vanadyl phosphate. *J. Solid State Electrochem.* **2004**, *8*, 322–329.
- (34) Johnson, J. W.; Jacobson, A. J.; Brody, J. F.; Rich, S. M. Coordination intercalation reactions of the layered compounds vanadyl phosphate (VOPO<sub>4</sub>) and vanadyl arsenate (VOAsO<sub>4</sub>) with pyridine. *Inorg. Chem.* **1982**, *21*, 3820–3825.
- (35) Igarashi, H.; Tsuji, K.; Okuhara, T.; Misono, M. Effects of consecutive oxidation on the production of maleic anhydride in butane oxidation over four kinds of well-characterized vanadyl pyrophosphates. *J. Phys. Chem.* **1993**, *97*, 7065–7071.
- (36) Chen, N.; Zhou, J.; Zhu, G.; Kang, Q.; Ji, H.; Zhang, Y.; Wang, X.; Peng, L.; Guo, X.; Lu, C.; Chen, J.; Feng, X.; Hou, W. A high-performance asymmetric supercapacitor based on vanadyl phosphate/carbon nanocomposites and polypyrrole-derived carbon nanowires. *Nanoscale* **2018**, *10*, 3709–3719.

(37) Dupré, N.; Gaubicher, J.; Le Mercier, T.; Wallez, G.; Angenault, J.; Quarton, M. Positive electrode materials for lithium batteries based on VOPO<sub>4</sub>. *Solid State Ionics* **2001**, *140*, 209–221.

(38) Park, J. G.; Aubrey, M. L.; Oktawiec, J.; Chakarawet, K.; Darago, L. E.; Grandjean, F.; Long, G. J.; Long, J. R. Charge Delocalization and Bulk Electronic Conductivity in the Mixed-Valence Metal-Organic Framework Fe (1, 2, 3-triazolate)<sub>2</sub>(BF<sub>4</sub>). *J. Am. Chem. Soc.* **2018**, *140*, 8526–8534.

(39) West, A. R. *Solid State Chemistry and Its Applications*; John Wiley & Sons, 2014; pp 102–104.

(40) Wei, Q.; Jiang, Z.; Tan, S.; Li, Q.; Huang, L.; Yan, M.; Zhou, L.; An, Q.; Mai, L. Lattice breathing inhibited layered vanadium oxide ultrathin nanobelts for enhanced sodium storage. *ACS Appl. Mater. Interfaces* **2015**, *7*, 18211–18217.

(41) Mizuno, Y.; Okubo, M.; Hosono, E.; Kudo, T.; Zhou, H.; Ohishi, K. Suppressed activation energy for interfacial charge transfer of a Prussian blue analog thin film electrode with hydrated ions (Li<sup>+</sup>, Na<sup>+</sup>, and Mg<sup>2+</sup>). *J. Phys. Chem. C* **2013**, *117*, 10877–10882.

(42) Hyoung, J.; Heo, J. W.; Chae, M. S.; Hong, S.-T. Electrochemical Exchange Reaction Mechanism and Role of Additive Water to Stabilize Structure of VOPO<sub>4</sub>·2H<sub>2</sub>O as a Cathode Material for Potassium-Ion Batteries. *ChemSusChem* **2019**, *12*, 1069–1075.

(43) Ji, X.; Chen, J.; Wang, F.; Sun, W.; Ruan, Y.; Miao, L.; Jiang, J.; Wang, C. Water-Activated VOPO<sub>4</sub> for Magnesium Ion Batteries. *Nano Lett.* **2018**, *18*, 6441–6448.

(44) He, P.; Quan, Y.; Xu, X.; Yan, M.; Yang, W.; An, Q.; He, L.; Mai, L. High-Performance Aqueous Zinc-Ion Battery Based on Layered H<sub>2</sub>V<sub>3</sub>O<sub>8</sub> Nanowire Cathode. *Small* **2017**, *13*, 1702551.

(45) He, P.; Zhang, G.; Liao, X.; Yan, M.; Xu, X.; An, Q.; Liu, J.; Mai, L. Sodium Ion Stabilized Vanadium Oxide Nanowire Cathode for High-Performance Zinc-Ion Batteries. *Adv. Energy Mater.* **2018**, *8*, 1702463.